scientific reports

Check for updates

OPEN

Establishment of an α-thalassemia mouse model through fetal liver cell transplantation and analysis of hematological parameters

Xin Xu[1,2], Wencheng Fu[1,2] & Wenrui Ye[1]✉

Clinically, α-thalassemia is stratified into mild, intermediate, and severe forms, differentiated by the degree of anemia severity. Specifically, severe α-thalassemia manifests in homozygous individuals, characterized by a profound α globin deficit. The presence of two α0 alleles, resulting in a complete four-gene defect ($\alpha^{--/--}$), constitutes a lethal in utero condition known as Hemoglobin (Hb) Barts hydrops fetalis syndrome. This arises from the inability of hemoglobin, deficient in α chains, to adequately transport oxygen. Consequently, this severe variant typically onsets during fetal development, often culminating in intrauterine death towards the end of gestation or dying shortly postpartum due to the compounded effects of severe anemia and resultant hypoxia. This study endeavors to establish an α-thalassemia mouse model via transplantation of embryonic liver cells harboring a dual α allele knockout, with a subsequent focus on comprehensively characterizing its hematological parameters and associated phenotypic indicators. To generate an α-globin chain-deficient mouse model, we transplanted fetal liver cells (harvested at embryonic day 13.5 from homozygous C57BL/6J-CD45.2-HBA-DKO mice) into C57BL/6 wild-type recipients preconditioned with 800 cGy irradiation. Multiple blood routine indicators, blood smear assessments, and spleen weight measurements, were subsequently conducted to characterize the model. Initially, model mice exhibited elevated white blood cell and lymphocyte counts relative to controls, potentially indicative of a possible immune reaction, though this response waned over time. Characteristic of the disease, these mice displayed significantly diminished mean corpuscular hemoglobin content and concentration, alongside heightened numbers of HbH inclusions and spleen weights. Furthermore, red blood cellindices, such as red blood cell count, hematocrit, red cell distribution width—coefficient of variation, and red cell distribution width—standard deviation, were all markedly increased in the model mice. Notably, model mice demonstrated significantly elevated values for mean platelet volume, platelet distribution width, and platelet large cell ratio percentage, reflective of aberrant platelet characteristics. Concurrently, a time-dependent increase in basophil percentages accompanied decreases in platelet count, platelet crit, and platelet larger cell count, collectively implying a progressively severe anemic state. Moreover, the progression from low to high levels of reticulocyte percentage and absolute reticulocyte count further corroborated an escalating tendency towards hemolysis. The model mice also experienced a substantial decline in body weight, underscoring the profound impact of disease progression on their health.

Keywords Athalassemia mouse model, Fetal liver cells transplantation, Hematological parameters, MCH, MCHC, HbH inclusion bodies

Alpha-thalassemia, a hereditary hematological disorder, arises from diminished α-globin chain production, causing an α-to-β globin imbalance that leads to a spectrum of pathologies, including ineffective erythropoiesis, curtailed red blood cell longevity, chronic hemolysis, and attendant complications[1]. Clinical presentations span from asymptomatic carriage to severe, transfusion-dependent conditions or fatality, largely contingent upon the underlying genotype. With 5–20% of the global population estimated to carry one or more α-thalassemia mutations, the disease constitutes a substantial worldwide health burden[2]. Amplified by extensive international

[1]Shanghai Pharma Rare Disease Medicine Co., Ltd., Shanghai 200000, China. [2]Xin Xu and Wencheng Fu contributed equally to this work. ✉email: yewenrui@sphchina.com

migration patterns in recent decades, α-thalassemia's prevalence has risen notably in regions historically less affected, such as Northern Europe and the Americas[3,4]. Barts hydrops fetalis syndrome (BHFS), also known as α-major thalassemia, represents the most severe clinical manifestation of α-thalassemia[5]. This condition arises when all four α globin genes are either deleted or rendered inactive, disrupting the normal transition from embryonic to fetal hemoglobin production. Consequently, the absence of fetal hemoglobin leads to a cascade of severe health issues, including progressive anemia, hepatosplenomegaly, and ultimately, heart failure[6]. Timely intervention via intrauterine blood transfusions is imperative to prevent fetal demise, typically between 23 and 38 weeks of gestation, or shortly post-birth[7–12]. For patients presenting with severe anemia (hemoglobin levels below 7 g/dL) associated with conditions like Hb Barts hydrops fetalis syndrome, the prevailing therapeutic approach involves regular blood transfusions. While intrauterine transfusions (IUTs) and intrauterine exchange transfusions (IUETs) offer a means for affected fetuses to survive the perinatal period, they introduce complex ethical considerations for both families and healthcare professionals[13]. Survivors of these interventions often necessitate lifelong blood transfusions, accompanied by the myriad complications that arise from chronic transfusion therapy[14]. Decisions surrounding the initiation of regular transfusions must weigh the substantial commitment to long-term care, the heightened risk of secondary iron overload and its associated complications, and the extensive utilization of medical resources. Thus, opting for a regimen of routine blood transfusions entails navigating a formidable array of challenges[15,16]. Hematopoietic stem cell transplantation (HSCT) has emerged as the sole curative therapy for thalassemia by virtue of its capacity to replace the hematopoietic system[17]. However, this intervention is fraught with risks and limited by the scarcity of compatible tissue donors for the majority of patients[18]. Despite recent advancements, α-thalassemia therapy continues to necessitate alternative strategies, all hinging upon the availability of a robust mouse model. At present, a satisfactory α-thalassemia mouse model remains elusive, although Stefano Rivella and colleagues recently announced at the European Hematology Association their development of such a model using embryonic liver transplanted with knockout α-genes[19]. While their announcement provided a brief outline of the model's physiological traits and claims of improvement through gene therapy, it lacked comprehensive details regarding the model's construction methodology. Although the Jackson Laboratory offers a homozygous Hba^{1-2del} mouse model (B6.129S7-Hbatm1Paz/J), this model results in in utero death and does not produce live, postnatal mice expressing the Hba^{1-2del} homozygous mutation, which are necessary for subsequent drug screening and the evaluation of therapeutic effects. This study aims to address this gap by meticulously delineating the methodology employed in generating an α-thalassemia mouse model via embryonic liver transplantation. It further furnishes exhaustive data on hematological parameters and a range of physiological indicators, thereby serving as a meticulous reference for future α-thalassemia research endeavors.

Results

In individuals with a normal genetic constitution, the presence of all four α-genes is typical. However, the absence of two α-genes results in the manifestation of α-thalassemia traits ($\alpha^{--/++}$). When both parents exhibit these traits, there exists a probability that their offspring will inherit haemoglobin Bart's hydrops foetalis syndrome (BHFS, $\alpha^{--/--}$). Initially, CRISPR/Cas9 technology was employed to engineer a mouse model lacking both Hba-a1 (E1-3) and Hba-a2 (E1-3) alleles on a single chromosome (Fig. 1A,B), constituting the F0 generation with α-thalassemia traits ($\alpha^{--/++}$). Proceeding from this, F0 generation females (13 mice) and males (13 mice), both harboring this trait, were mated to generate an F1 generation cohort (83 mice), amongst which a subset would inherit the BHFS.

Genotyping of F1 generation fetal mice was accomplished through polymerase chain reaction (PCR) analysis. Two primer pairs (designated F1R1 and F2R2) were strategically designed to verify the Hba-a1 (E1-3) and Hba-a2 (E1-3) alleles (Fig. 2A and Supplementary Table 1). Employing primer sets F1R1 and F2R2 tailored for Hba-a1 (E1-3), the absence of targeted bands in samples numbered 2–5, 3–1, 3–3, 4–3, 7–1 to 7–2, 8–2, 8–5, 9–6 to 9–8, 10–4 to 10–6, 11–3, 12–7, 13–1 to 13–3, and 13–5 signified deletions within the Hba-a1 (E1-3) gene (Fig. 2B,C). Similarly, when applying primer sets F1R1 and F2R2 designed for Hba-a2 (E1-3), the lack of target

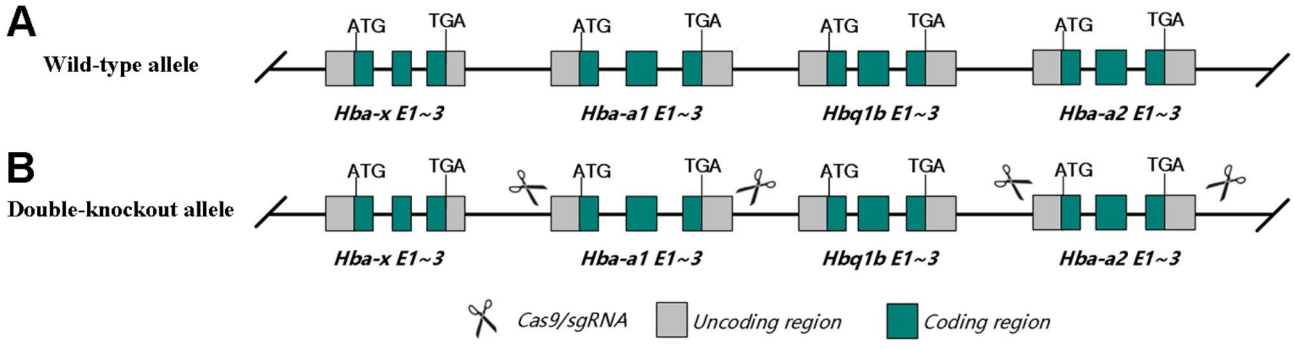

Fig. 1. Schematic diagram showing the strategy to double knockout the mouse Hba-a1 (E1-3) and Hba-a2 (E1-3) genes via CRISPR/Cas9 system. (**A**) The wild type (WT) architecture of the mouse Hba-a1 (E1-3) and Hba-a2 (E1-3) alleles. (**B**) The modified structure of the mouse Hba-a1 (E1-3) and Hba-a2 (E1-3) alleles subsequent to targeting by the CRISPR/Cas9 system.

bands in specimens numbered 2–5, 3–1, 3–3, 4–3, 7–1 to 7–2, 8–2, 8–5, 9–3, 9–6 through 9–8, 10–4 to 10–6, 10–12, 11–3, 12–7, 12–9, 13–1, 13–2, and 13–5 confirmed deletions in the Hba-a2 (E1-3) gene (Fig. 2D,E). Consolidating these findings, we verified that the fetal mice bearing identification numbers 2–5, 3–1, 3–3, 4–3, 7–1 to 7–2, 8–2, 8–5, 9–3, 9–6, 9–7, 9–8, 10–4 to 10–6, 10–12, 11–3, 12–7, 12–9, 13–1, 13–2, and 13–5 harbor homozygous deletions in both Hba-a1 (E1-3) and Hba-a2 (E1-3) alleles, confirming their (22 fetal mice) status as double-knockout mice for these alleles.

Following genotyping of the F1 generation, we procured fetal liver cells from homozygous fetuses ($\alpha^{--/--}$) and utilized them in establishing an adult mouse model devoid of all four α-globin genes by means of injecting these cells into CD45.1 mice (5 mice per group) with 800 cGy irradiation via the tail vein. All mice in the study survived. Hematological assessments, including complete blood counts, were conducted on the modeled mice at intervals of 28, 42, and 56 days post-procedure (Fig. 3 and Supplementary Table 2).

Our findings revealed a distinctive pattern in the α-thalassemia mouse model: White blood cell (WBC) counts were notably elevated compared to the control group at the initial assessment on day 28, but progressively decreased over time until day 56. Lymphocyte counts exhibited a parallel trajectory, declining from significantly higher levels than the control to levels indistinguishable from the control by day 56, albeit with an initial increase in the lymphocyte percentage from significantly lower to non-significantly different than the control. This trend suggests an obvious initial immune response followed by a diminution over time. What's more, Ali et al. reported that higher levels of TNF-α, IL-1β, IL-6, IL-8, and C-reactive protein, which are proinflammatory cytokines, have been observed in the serum of patients with thalassemia major (TM). Additionally, TM patients exhibited increased ratios of regulatory B lymphocytes (CD19+, CD38+, CD24+), helper T cells, suppressor T cells, and T regulatory (CD4+/CD25+/Foxp3+) lymphocytes[20]. Meanwhile, Gharagozloo et al. reported that elevated ferritin levels were associated with decreased levels of IFN-γ and IL-2 in subjects, indicating an immune suppressive effect of iron overload in β-thalassemia patients[21]. We hypothesize that the initially observed significantly higher levels of white blood cells and lymphocytes in the α-thalassemia model group, compared to the control group, may be due to immune system activation. However, over time, iron overload resulting from red blood cell hemolysis may lead to a significant decrease in these levels. These align with the observed hematological dynamics.

Significantly elevated levels were observed in RBC counts, HCT, RDW_CV, and RDW_SD compared to controls, aligning with documented clinical manifestations akin to beta-thalassemia (referenced elsewhere). Conversely, MCH and MCHC were notably reduced. Hemoglobin (HGB) and mean corpuscular volume (MCV) values exhibited a recovery trend from the 28th to the 56th day, suggestive of erythrocyte compensatory mechanisms, culminating in a significant total hemoglobin increase despite persistently low MCH compared to controls. MPV, PDW, and P_LCR percentage also surpassed control levels, accompanied by a gradual rise in Bas percentage and declines in PLT, PCT, and P_LCC, collectively pointing to aberrant platelet function and progressing anemia. The progressive elevation of RETI percentage and RETI_ABS from the 28th to the 56th day further implied an escalating risk of hemolysis. Notably, the proportions of monocytes (Mon), neutrophils (Neu), eosinophils (Eos), and the immature reticulocyte fraction (IRF), as well as the concentrations of Monocytes and Eosinophils, remained unaltered amidst these alterations.

Concurrently, HbH inclusion bodies were assayed via Brilliant Cresyl Blue staining at 28 (Fig. 4A–C), 42 (Fig. 4D–F), and 56 days (Fig. 4G–I) post-intervention, revealing a marked elevation compared to controls, thereby further substantiating the occurrence of β-globin tetramer formation in the model mice. Mice were weighed twice-weekly, and from day 35 onwards, their weights were significantly reduced relative to controls, exhibiting a persistent decrement (Fig. 4J). By day 56, the weight loss demonstrated a highly statistically significant difference from the control group ($p < 0.0001$). While the models' body weight was strikingly lower than the controls on day 56, their spleen weight was disproportionately higher (~8-fold), reflecting the characteristic splenomegaly associated with α-thalassemia (Fig. 4K).

Prior to the experiment's commencement, a preliminary trial was undertaken, wherein both the model and wild-type groups recorded a GVHD score of 0 throughout the initial 22 days (Supplementary Fig. 1A). Notably, the control group, subjected solely to irradiation sans fetal liver cell transplantation, succumbed on day 15, effectively excluding the likelihood of GVHD induced by our methodology. Complementary to this, flow cytometry (FACS) analysis confirmed the expression profiles of mCD45.1+ and mCD45.2+ (Supplementary Fig. 1B). This evidenced the establishment of a chimeric blood phenotype three weeks post-transplantation, characterized by an approximate 85% proportion of mCD45.2+ cells and 10% of mCD45.1+ cells.

Discussion

Our study has validated the efficacy of fetal liver cell transplantation in adult mice, successfully establishing an α-thalassemia murine model. Temporally, a decline in WBC and Lym numbers in model mice is evident, indicative of an initially obvious immune response that wanes over time. Persistent and significant reductions in MCH and MCHC, concurrent with HbH inclusion body formation, progressive weight reduction, and splenomegaly, mirror key clinical features observed in thalassemia patients. Aberrations in basophil counts, platelet parameters (PLT, MPV, PDW, P_LCC, P-LCR), and PCT collectively imply advancing anemia. Furthermore, heightened RBC counts, RETIC percentage, and RETIC_ABS in model mice, surpassing control levels, potentially signify compensatory hematopoiesis.

In conclusion, α-thalassemia is a blood disorder, and we have developed an adult α-thalassemia mouse model using fetal liver cells with targeted knockouts in both Hba-a1 (E1-3) and Hba-a2 (E1-3) alleles. This model mimics the pathophysiology of severe human α-thalassemia. Our work provides a detailed methodology for constructing this severe α-thalassemia mouse model, enabling other researchers to replicate it for further studies. We also present comprehensive data on hematological parameters, HbH inclusion bodies, and body

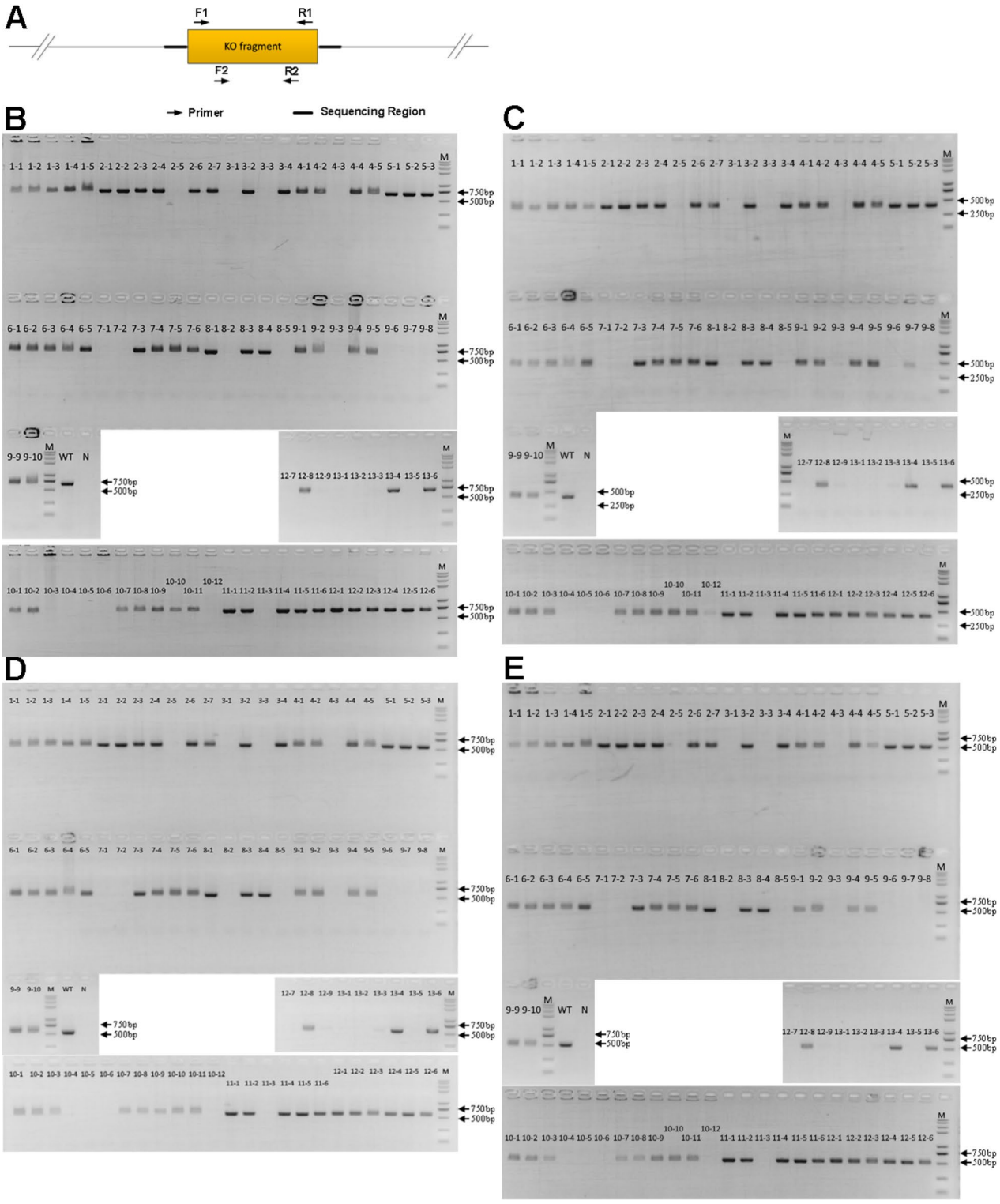

weight changes over time, as well as information on kidney weight differences, providing a valuable resource for research into α-thalassemia and its treatments.

Methods

Mouse model of α-thalassemia

The Jicui Pharmaceutical Group supplied and maintained the breeding of C57BL/6JGpt-CD45.1 and C57BL/6J-CD45.2 mice. To obtain fetal mice, pregnancies in C57BL/6J-CD45.2-HBA-DKO mice at 13.5 days of gestation were terminated via euthanasia. Following abdominal sterilization, surgical access was gained to the uterus, which was then extracted. Fetal mice were harvested and promptly transferred to a 6-well plate with DPBS/0.02% BSA solution for a 20-min incubation. For swift genotyping (completed within approximately 4–5 h), a tail segment from each fetus was carefully excised, ensuring no maternal blood contamination, and immersed in DPBS.

◀**Fig. 2**. PCR-Based Identification of Hba-a1 (E1-3) and Hba-a2 (E1-3) Allele-Targeted Fetal Mice. (**A**) The diagram illustrates the strategic placement of two PCR primer pairs utilized for genotyping. (**B**) PCR outcomes for Hba-a1 (E1-3) allele-targeted fetuses, amplified with Hba-a1:F1R1 primers, where wild-type and double knockout alleles yield bands of 659 bp and 0 bp, respectively. (**C**) PCR results for the same Hba-a1 (E1-3) allele using Hba-a1:F2R2 primers, exhibiting band sizes of 390 bp for wild type and 0 bp for double knockouts. (**D**) PCR screenings for Hba-a2 (E1-3) allele-targeted fetuses using Hba-a2:F1R1 primers, with band sizes of 538 bp for wild type and 0 bp indicative of double knockouts. (**E**) PCR outcomes for Hba-a2 (E1-3) allele knockouts utilizing Hba-a2:F2R2 primers, differentiating wild type (491 bp) from double knockouts (0 bp) bands. Note: Numbering System: The first digit in the number (e.g., 1–1) represents the pregnant mouse's ID, and the second digit represents the offspring's ID. For example, 1–1 and 1–2 refer to the first and second offspring of pregnant mouse 1, respectively. This pattern applies to all other numbers. *WT* wild type control, *N* null control, *M* marker.

The C57BL/6JGpt-CD45.1 and C57BL/6J-CD45.2 mouse strains were bred and supplied by Jicui Pharmaceutical for the study. Initially, CRISPR/Cas9 technology accompanied by PCR-based genotyping was employed to establish a line of mice with knockouts of Hba-a1 (E1-3) and Hba-a2 (E1-3) alleles on a single chromosome, designated as F0 generation (C57BL/6J-CD45.2-HBA-DKO, $a^{++/--}$). Subsequently, mating between heterozygous F0 females ($a^{++/--}$) and males of the same genotype was conducted to produce F1 offspring with a likelihood of harboring the $a^{--/--}$ homozygous knockout genotype.

To obtain fetal mice, pregnancies in C57BL/6J-CD45.2-HBA-DKO mice at 13.5 days of gestation were terminated via euthanasia. Following abdominal sterilization, surgical access was gained to the uterus, which was then extracted. Fetal mice were harvested and promptly transferred to a 6-well plate with DPBS/0.02% BSA solution for a 20-min incubation. For swift genotyping (completed within approximately 4–5 h), a tail segment from each fetus was carefully excised, ensuring no maternal blood contamination, and immersed in DPBS.

DNA was extracted using alkaline lysis, and genotyping was performed by PCR with two distinct primer pairs specifically designed for the identification of both wild-type (WT) and C57BL/6J-CD45.2-HBA-DKO alleles. Concurrently, fetal livers were harvested for subsequent processing. These livers were immersed in cold DPBS/0.02% BSA solution within a 6-well plate and dissociated into single-cell suspensions utilizing a 40 μm cell strainer. Cell counts were performed, and suspensions adjusted to 1×10^7 cells/ml in DPBS, held in readiness pending genotyping outcomes (within a 5-hour timeframe). Mice were stratified into groups randomly based on their weights prior to irradiation. The C57BL/6JGpt-CD45.1 strain received a radiation dose of 800 cGy delivered at 1 Gy/min. A prophylactic antibiotic regimen was initiated one week before irradiation and sustained for an additional two weeks post-treatment. Designating the day of irradiation and group allocation as Day 0, mice underwent transplantation 2–4 h post-irradiation, receiving 1×10^6 fetal liver cells in 100 μL via intravenous injection. Observations were conducted daily, and mice were weighed twice weekly. At specified time points (Day 28, Day 42, and Day 56), 50–70 μL of EDTA-anticoagulated peripheral blood was sampled to perform complete blood counts, including analyses of red blood cells, platelets, hemoglobin, reticulocyte counts, among other parameters. Subsequently, the animals were humanely euthanized at day 56 using isoflurane and their spleens were harvested for weighing.

Brilliant cresyl blue staining

Combine the Brilliant Cresyl Blue (BCB) solution (mlbio) with mouse whole blood at a 2:1 ratio, seal the vessel, and incubate in a 37 °C water bath for a duration of 4 to 18 h. Proceed to prepare standard blood smears, which are then examined microscopically. Alternatively, enumerate 600 red blood cells under oil immersion, noting that positive cells exhibit dark green-blue, variably sized and numerous, irregularly dispersed intracellular inclusions, indicative of hemoglobin H inclusion bodies. Subsequently, determine the proportion of red blood cells positive for HbH inclusion bodies.

Genotyping of fetal mice via PCR

A segment of the fetal mouse tail is excised and rinsed in DPBS solution before being transferred to a 1.5 mL EP tube. Next, 100 μL of Solution A, composed of 0.1 g NaOH, 0.058 g EDTA in 100 mL ddH_2O, is introduced for thorough mixing, followed by centrifugation. The mixture is subsequently incubated at 100 °C in a metal bath for an hour, undergoing one mid-cycle remixing and centrifugation. Upon cooling to ambient temperature, 100 μL of Solution B (prepared with 0.63 g Trizma base in 60 mL ddH_2O) is added and thoroughly mixed, rendering the sample suitable for genotyping through utilization of a Taq PCR Kit. The PCR protocol entails an initial denaturation at 95 °C for 30 s, succeeded by 30 repetitive cycles comprising 20 s at 95 °C, 30 s at a temperature range of 45–68 °C, and 1 min per base pair at 68 °C, culminating in a final extension step at 72 °C for 5 min. Thereafter, the PCR products are resolved on a 1% agarose gel. Gel electrophoresis is performed, and the resultant band patterns are visualized using a gel documentation system (Tanon) to ascertain the fetal mouse genotypes.

Hematological parameter assessment

Hematological analyses were conducted employing an automated analyzer, URIT (China). This URIT is a five-part differential hematology analyzer employing four-angle laser scattering technology, which can accurately classify WBCs into five categories and effectively exclude the influence of abnormal cells such as nucleated red blood cells, poorly lysed red blood cells, fragile leukocytes, and aggregated platelets. The comprehensive panel encompassed key parameters such as total white blood cell count (WBC), differential counts including basophils

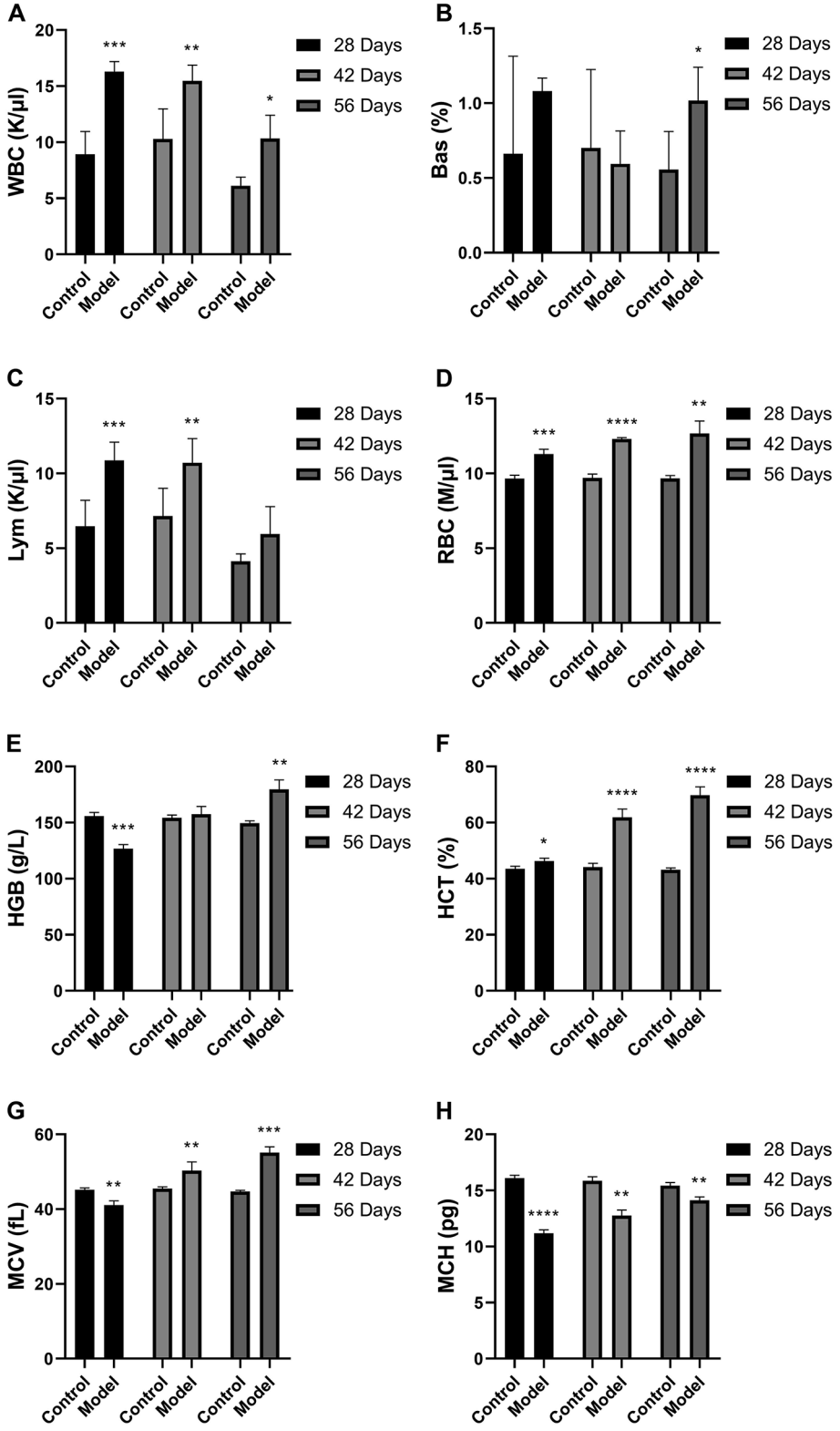

Fig. 3. Hematological parameters of the α-thalassemia mouse model. Data are presented as mean ± SD (n = 5 per group), representing the following parameters: (**A**) white blood cell count (WBC), (**B**) basophils (Bas), (**C**) lymphocytes (Lym), (**D**) red blood cells (RBC), (**E**) hemoglobin (HGB), (**F**) hematocrit (HCT), (**G**) mean corpuscular volume (MCV), (**H**) mean corpuscular hemoglobin (MCH), (**I**) mean corpuscular hemoglobin concentration (MCHC), (**J**) red cell distribution width-standard deviation (RDW_SD), (**K**) platelet count (PLT), (**L**) mean platelet volume (MPV), (**M**) platelet distribution width (PDW), (**N**) platelet crit (PCT), (**O**) larger platelet count (P_LCC), and (**P**) absolute reticulocyte count (RETIC_ABS). Statistically tested with a paired t-test. Significance levels: $^{*}P < 0.05$, $^{**}P < 0.01$, $^{***}P < 0.001$, $^{****}P < 0.0001$ denote statistically significant differences.

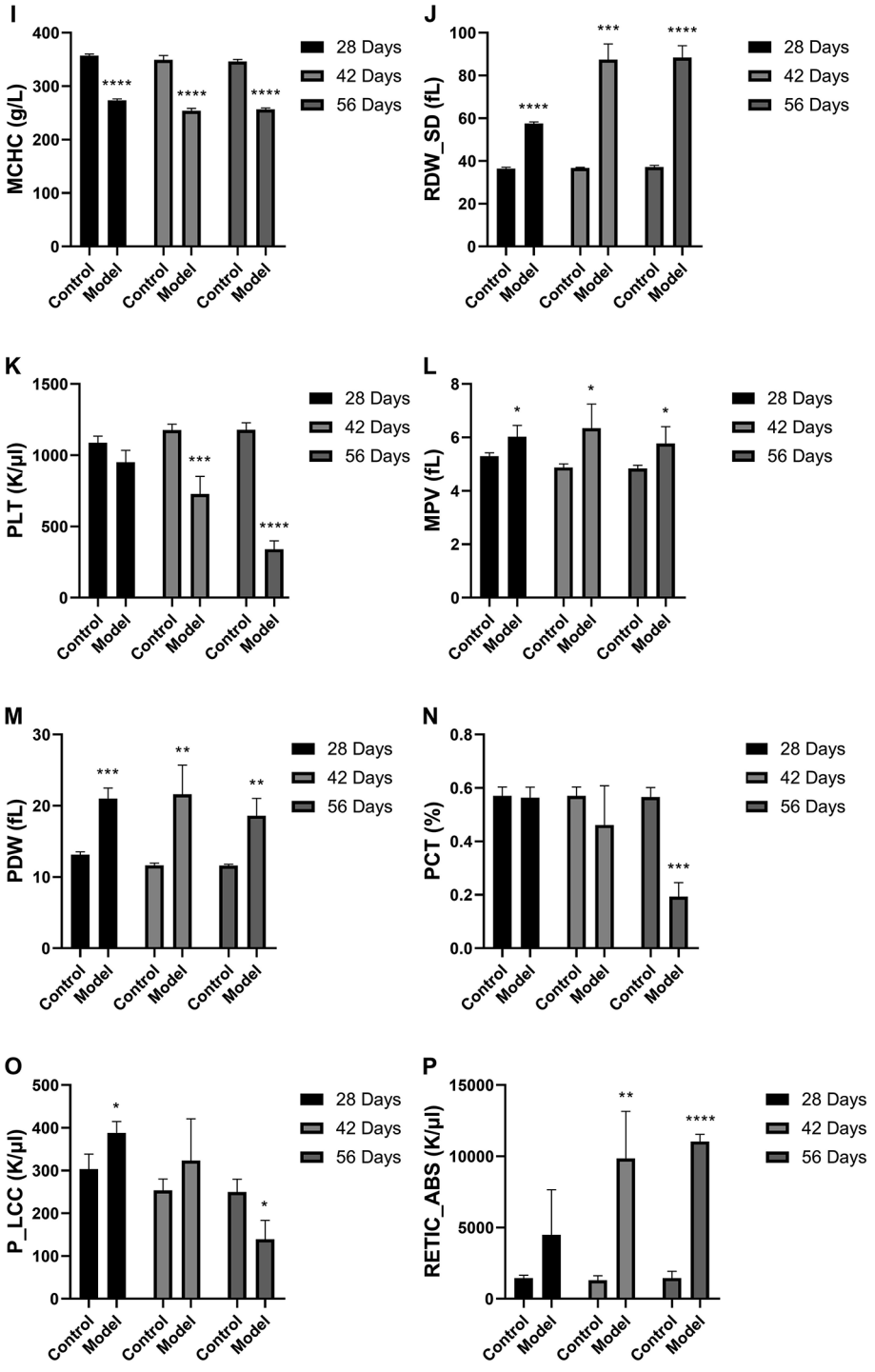

Figure 3. (continued)

(Bas), lymphocytes (Lym), red blood cells (RBC), hemoglobin (HGB), hematocrit (HCT), mean corpuscular volume (MCV), mean corpuscular hemoglobin (MCH), mean corpuscular hemoglobin concentration (MCHC), red cell distribution width standard deviation (RDW_SD), platelet count (PLT), mean platelet volume (MPV), platelet distribution width (PDW), platelet crit (PCT), platelet larger cell count (P_LCC), absolute reticulocyte count (RETIC_ABS), monocytes (Mon), neutrophils (Neu), eosinophils (Eos), red cell distribution width coefficient of variation (RDW_CV), platelet large cell ratio percentage (P_LCR %), reticulocyte count percentage (RETI %), immature reticulocyte fraction (IRF), among others.

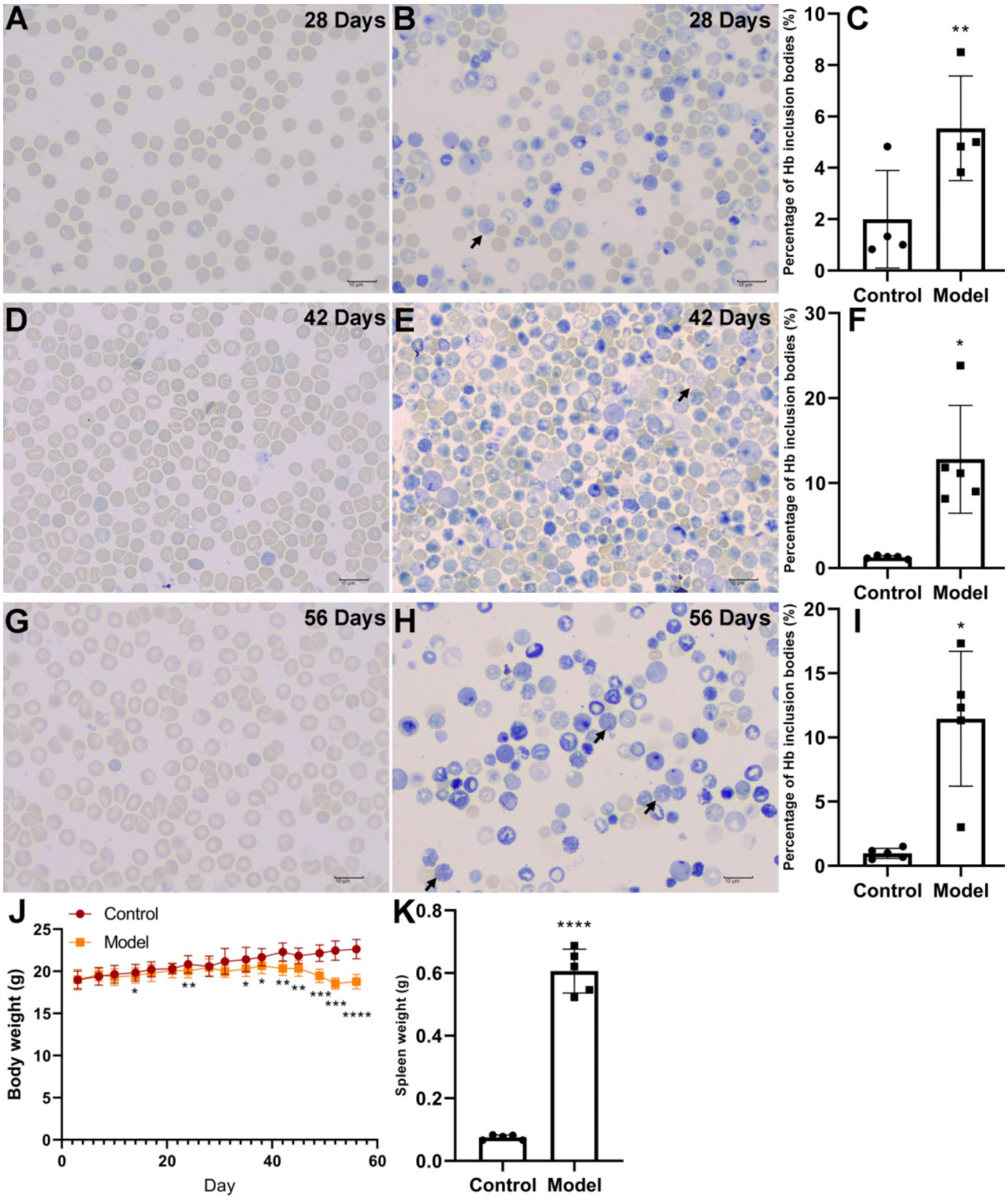

Fig. 4. HbH Inclusion Bodies Observation and Quantification in an α-Thalassemia Murine Model. HbH inclusion bodies, visualized on BCB-stained blood smears, are depicted at 28 days (**A**,**B**), 42 days (**D**,**E**) and 56 days (**G**,**H**). (**C**) Quantification of (**A**) and (**B**) (n = 12) presented as mean ± SD. (**F**) Quantification of (**D**) and (**E**) (n = 15) presented as mean ± SD. (**I**) Quantification of (**G**) and (**H**) (n = 15) presented as mean ± SD. (**J**) The changes in body weight twice-weekly. (**K**) The spleen weight on day 56. Statistically tested with a paired t-test, $^{*}P < 0.05$, $^{**}P < 0.01$, $^{***}P < 0.005$, $^{****}P < 0.001$ between control and model groups.

Statistical analysis
All data were collated in GraphPad Prism 8 which was also used for statistical analysis. All data are presented as mean ± standard deviation (SD). A paired two-tailed t-test was performed to determine the level of significant difference between control and model groups. $^{*}P<0.05$, $^{**}P<0.01$, $^{***}P<0.001$, $^{****}P<0.0001$.

Data availability
The datasets used and analysed during the current study available from the corresponding author on reasonable request.

Received: 8 July 2024; Accepted: 24 February 2025
Published online: 28 February 2025

References
1. Muncie, H. L. et al. Alpha and beta thalassemia. *Am. Fam. Physician* **80**, 339–344 (2009).
2. Musallam, K. M. et al. Alpha-thalassemia: A practical overview. *Blood Rev.* **64**, 101165 (2024).
3. Angastiniotis, M. et al. The impact of migrations on the health services for rare diseases in Europe: The example of haemoglobin disorders. *Sci. World J.* **2013**, 727905 (2013).
4. Weatherall, D. J. The evolving spectrum of the epidemiology of thalassemia. *Hematol. Oncol. Clin. N. Am.* **32**, 165–175 (2018).
5. Songdej, D. et al. An international registry of survivors with Hb Bart's hydrops fetalis syndrome. *Blood* **129**, 1251–1259 (2017).
6. Vanaparthy, R. et al. *Hydrops Fetalis* (StatPearls Publishing, 2022).
7. Chan, W. Y. et al. Outcomes and morbidities of patients who survive haemoglobin Bart's hydrops fetalis syndrome: 20-year retrospective review. *Hong Kong Med. J.* **24**, 107–118 (2018).
8. Yi, J. S. et al. Homozygous alpha-thalassemia treated with intrauterine transfusions and unrelated donor hematopoietic cell transplantation. *J. Pediatr.* **154**, 766–768 (2009).
9. Lee, S. Y. et al. Outcome of intensive care of homozygous alpha-thalassaemia without prior intra-uterine therapy. *J. Paediatr. Child Health* **43**, 546–550 (2007).
10. Shirasawa, T. et al. Oxygen affinity of hemoglobin regulates O_2 consumption, metabolism, and physical activity. *J. Biol. Chem.* **278**, 5035–5043 (2003).
11. McKie, K. M. et al. Postnatal changes in the quantities of globin chains and hemoglobin types in two babies with Hb H disease. *Am. J. Hematol.* **42**, 86–90 (1993).
12. Pászty, C. et al. Lethal alpha-thalassaemia created by gene targeting in mice and its genetic rescue. *Nat. Genet.* **11**, 33–39 (1995).
13. Fung, T. Y. et al. In utero exchange transfusion in homozygous alpha-thalassaemia: A case report. *Prenat. Diagn.* **18**, 838–841 (1998).
14. Trachtenberg, F. L. et al. Relationship among chelator adherence, change in chelators, and quality of life in thalassemia. *Qual. Life Res.* **23**, 2277–2288 (2014).
15. Cappellini, M. D. et al. *2021 Guidelines: For the Management of Transfusion Dependent Thalassaemia (TDT)* 4th edn. (Thalassaemia International Federation, 2023).
16. Lal, A. et al. Transfusion practices and complications in thalassemia. *Transfusion* **58**, 2826–2835 (2018).
17. Algeri, M. et al. Hematopoietic stem cell transplantation in thalassemia. *Hematol. Oncol. Clin. N. Am.* **37**, 413–432 (2023).
18. Bozkurt, G. Results from the north cyprus thalassemia prevention program. *Hemoglobin* **31**, 257–264 (2007).
19. Rivella, S. et al. P1521: A Sever mouse model of alpha-thalassemia shows abnormal iron metabolism, erythropoiesis and coagulation, and can be rescued by a novel gene therapy approach. *HemaSphere* **6**, 1402–1403 (2022).
20. Ali, B. et al. The role of immune system in thalassemia major: A narrative review. *J. Pediatr. Rev.* **6**, e14508 (2018).
21. Gharagozloo, M. et al. Double-faced cell-mediated immunity in beta-thalassemia major: Stimulated phenotype versus suppressed activity. *Ann. Hematol.* **88**, 21–27 (2009).

Acknowledgements
This work was also supported by Shanghai Pharma. We thank members of the GemPharmatech Co., Ltd for technical assistance; Jiale Chen for irradiation; Hui Yang, Chuqian Shi, Wen Xie and colleagues provided technical support for the α-thalassemia mouse model.

Author contributions
X.X., W.F. and W.Y. designed this project and completed this article. X.X. and W.Y. also supervised the project, while W.Y. and W.F. conducted the experiments involving the α-thalassemia mouse model. X.X. and W.F. wrote the manuscript. All the authors have read and approved the final manuscript.

Funding
Shanghai Pharma Rare Disease Medicine Company.

Declarations

Competing interests
The authors declare no competing interests.

Ethical approval
All animal experiments were conducted in accordance with the ARRIVE Guidelines, the Guide for the Care and Use of Laboratory Animals (https://grants.nih.gov/grants/olaw/guide-for-the-care-and-use-of-laboratory-animals.pdf), and the Institutional Animal Care and Use Committee (IACUC) of Gempharmatech Co., Ltd., following approval by the Animal Ethics Committee (GPTAP20231109-6). To thoroughly consider the ethical implications of using fetal liver cells for transplantation, we evaluated several alternative methods before selecting fetal liver cells as the experimental material. While adult stem cells and other cell types can be used in some studies, fetal liver cells offer unique advantages in mimicking the pathophysiology of human

α-thalassemia. Fetal liver cells contain a high number of hematopoietic stem cells, which more accurately reflect the disease state. The aim of this study is to develop a new mouse model to better understand the pathogenic mechanisms of α-thalassemia and provide a platform for future therapeutic strategies. This model will enable us to investigate the molecular mechanisms of the disease and test potential treatments, particularly gene therapy. We believe that the potential scientific and societal benefits of this research outweigh the ethical risks.

Additional information

Supplementary Information The online version contains supplementary material available at https://doi.org/10.1038/s41598-025-91792-5.

Correspondence and requests for materials should be addressed to W.Y.

Reprints and permissions information is available at www.nature.com/reprints.

Publisher's note Springer Nature remains neutral with regard to jurisdictional claims in published maps and institutional affiliations.